Available online at www.sciencedirect.com
SCIENCE DIRECT®
Thermochimica Acta 430 (2005) 183–190
thermochimica acta
www.elsevier.com/locate/tca

Melting and thermal history of poly(hydroxybutyrate-co-hydroxyvalerate) using step-scan DSC

L.M.W.K. Gunaratne, R.A. Shanks *

School of Applied Science, RMIT University, GPO Box 2476V, Melbourne, Vic. 3001, Australia

Received 29 October 2004; received in revised form 18 January 2005; accepted 26 January 2005
Available online 17 February 2005

Abstract

Melting behaviour and crystal morphology of poly(3-hydroxybutyrate) (PHB) and its copolymer of poly(3-hydroxybutyrate-co-3-hydroxyvalerate) with various hydroxyvalerate (HV) contents [5 wt.% (PHB5HV), 8 wt.% (PHB8HV) and 12 wt.% (PHB12HV)] have been investigated by conventional DSC, step-scan differential scanning calorimetry (SDSC) and hot-stage polarised optical microscopy (HSPOM). Crystallisation behaviour of PHB and its copolymers were investigated by SDSC. Thermal properties were investigated after different crystallisation treatments, fast, medium and slow cooling. Multiple melting peak behaviour was observed for all polymers. SDSC data revealed that PHB and its copolymers undergo melting–recrystallisation–remelting during heating, as evidenced by exothermic peaks in the IsoK baseline (non-reversing signal). An increase in degree of crystallinity due to significant melt–recrystallisation was observed for slow-cooled copolymers. PHB5HV showed different crystal morphologies for various crystallisation conditions. SDSC proved a convenient and precise method for measurement of the apparent thermodynamic specific heat (reversing signal) HSPOM results showed that the crystallisation rates and sizes of spherulites were significantly reduced as crystallisation rate increased.

Keywords: Step-scan DSC; Poly(hydroxybutyrate); Crystallization; Melting; Morphology

1. Introduction

Poly(3-hydroxybutyrate) (PHB) and its copolymers with 3-hydroxyvalerate (HV) having chemical structures of $[-OCH(CH_3)CH_2(C=O)-]_n$ and $[-OCH(CH_3)CH_2(C=O)-]_x[-OCH(C_2H_5)CH_2(C=O)-]_y$ respectively are synthesised by bacteria. In addition to biosynthesis, they have attracted much interest because of their biocompatibility and biodegradability. They have relatively high melting temperatures (T_m), up to 170 °C for the homopolymer [1,2]. Their relatively high glass transition temperatures (T_g) and crystallinity have made them too brittle for many applications. The copolymers have more suitable T_g, but they are slow to reach crystallisation equilibrium. They crystallise slowly to form large crystals. Their continuing interest as biopolymers and their slow crystallisation equilibration have made them the subject of many crystallisation studies [3].

Differential scanning calorimetry (DSC) is a valuable technique to study melting and crystallisation behaviour of polymers. The interpretation of DSC results is difficult due to various transformations occurring simultaneously during heating. Temperature modulated differential scanning calorimetry (TMDSC) has attracted much interest since its development in 1992, because of its ability to distinguish apparent thermodynamic (reversing signal) and kinetic (non-reversing signal) events under the prevailing DSC modulation conditions [4–6]. The theory and operating principles have been thoroughly described [4–9].

Three types of curves can be derived from the experiments: total heat flow or heat capacity curve (total C_p, the same as a conventional DSC curve), the in-phase curve (reversing or storage) and out-of-phase curve (loss) [10]. In addition a non-reversing heat capacity (kinetic) curve can be obtained from the difference between the total and reversing C_p.

* Corresponding author. Tel.: +61 3 9925 2122; fax: +61 3 9639 1321.
E-mail address: robert.shanks@rmit.edu.au (R.A. Shanks).

0040-6031/$ – see front matter © 2005 Elsevier B.V. All rights reserved.
doi:10.1016/j.tca.2005.01.060

Another TMDSC method, called step-scan DSC (SDSC) has recently become available [11]. SDSC utilises a heat–isothermal (or cool–isothermal) program, where the isothermal segment continues for a set time and heat flow is decreased to within a predetermined set-value (criteria). The apparent thermodynamic response only occurs during the heating (or cooling) segment and reflects the reversing changes within the sample. The time-dependent response reflects the kinetic processes and is extracted from the isothermal baseline segment. The equation that describes the heat flow response is given by

$$dQ/dt = C_p(dT/dt) + f(t, T)$$

where dQ/dt is the heat flow, C_p the heat capacity, dT/dt the heating rate and $f(t,T)$ the kinetic response. The interpretation of results is similar to other forms of TMDSC. Analysis of the heat flow signal provides two curves: the apparent thermodynamic C_p ($C_{p,\mathrm{ATD}}$) signal (reversible under the experimental conditions or reversing) and the IsoK baseline C_p ($C_{p,\mathrm{IsoK}}$) (kinetic or non-reversing) curves. We have chosen to define these terms in this way since the Perkin-Elmer definition of 'thermodynamic specific heat' creates some controversy in that it is not a true thermodynamic parameter, yet it is obtained differently from the other reversing heat flow or capacity obtained from TMDSC methods. A Fourier transformation is not involved for the heat capacity calculation from SDSC heat flow as for other TMDSC methods and the method is free of experimental problems such as thermal gradients, sine wave distortions or phase lag [12].

The aim of this work is to study the influence of thermal history of PHB copolymers with HV (PHBHV) using a range of non-isothermal crystallisation conditions. The melting of PHB and its copolymers is studied using the SDSC technique. SDSC has recently been used to characterise polyanhydrides [13] pigments [11] and poly(ethylene oxide) [12]. A morphological study of PHBHV is carried out using HSPOM with crystallisation conditions related to the DSC cooling treatments.

2. Experimental

2.1. Sample preparation

Bacterial PHB and poly(3-hydroxybutyrate-co-3-hydroxyvalerate) with various HV contents [5 wt.% (PHB5HVA), 8 wt.% (PHB8HV) and 12 wt.% (PHB12HV)] were obtained from Sigma-Aldrich Chemicals as white powders ($M_w = 2.3 \times 10^5$ g mol^{-1} and $M_n = 8.7 \times 10^4$ g mol^{-1} [14] of PHB). Polymer (1 g) was dissolved in 100 mL of chloroform and filtered under vacuum to remove any insoluble fraction or impurities. Semi-crystalline films were obtained by solvent casting at room temperature. The resulting films were further dried in vacuum at 50 °C for 3 h to remove any a residual solvent and moisture. Films were stored in desiccator under nitrogen atmosphere prior to use.

2.2. SDSC method and data analysis

All measurements and thermal treatments were performed using a Perkin-Elmer series Pyris 1 DSC (Pyris software 3.81) operated in subambient temperature mode with an Intracooler 2P. About 2–3 mg of polymer was sealed in a 10 μL aluminium pan, and all scans were carried out under inert nitrogen (20 mL min^{-1}). High purity indium and octadecane were used for temperature calibration and indium standard was used for calibration of heat flow. The furnace was calibrated according to the manufacture recommendation. Specific heat capacity results were calibrated using a sapphire standard.

The SDSC melting scans of samples with controlled thermal history were obtained with an average heating rate of 2 °C min^{-1} and a period of 60 s (a temperature increment of 2 °C with each 30 s scanning segments) from −20 to 190 °C. Each polymer was heated to the melt at 190 °C for 3 min to remove any prior thermal history. The PHB5HV were treated by cooling at 200, 20 and 2 °C min^{-1} rates. Specific heat calculation from heat flow response of the SDSC scans was carried out using the area method. The data for each isothermal segment was collected to within a 0.005 mW s^{-1} baseline criteria. The heat flow data from the SDSC scans were used to calculate the apparent thermodynamic heat capacity ($C_{p,\mathrm{ATD}}$) and IsoK baseline heat capacity ($C_{p,\mathrm{IsoK}}$). All SDSC curves were corrected using an appropriate baseline recorded under identical conditions with matched empty aluminium pans when converting to specific heat capacity curves. From the SDSC heating scans, glass transition temperature (T_g), cold crystallisation temperature (T_{cc}), melting temperature (T_m) and enthalpy of fusion (ΔH_m) were determined.

The crystallinity was calculated using the equation:

$$X_c = \Delta H_m / \Delta H^\circ_{\mathrm{PHB}}$$

where $\Delta H^\circ_{\mathrm{PHB}}$ is the enthalpy of melting of pure PHB crystals 146 J g^{-1} [15] and ΔH_m the measured enthalpy of melting for each polymer.

2.3. Optical microscopy

The crystal morphologies of PHB5HV copolymer were observed using a Nikon Labophot 2 polarising optical microscope with a Mettler FP90 hot stage and images were captured using a Nikon digital camera. Each film was mounted on a glass slide under a cover slip. The specimens were first heated on a hot-stage from room temperature to 190 °C at a rate of 5 °C min^{-1} and maintained at this temperature for 3 min before cooling. The morphological study of PHB5HV was carried out using three different crystallisation conditions: isothermal crystallisation, continuous slow and fast cooling rates from 140 °C to room temperature after cooling to 140 °C at 5 °C min^{-1} under

nitrogen atmosphere. Isothermal crystallisation behaviour was observed by maintaining the sample for one hour at 80 °C after cooling at 5 °C min^{-1} from 190 °C. Cooling rates of 20 and 2 °C min^{-1} were used to provide analogous behaviour to the DSC treatment of the polymers.

3. Results and discussion

3.1. Evaluation of SDSC results

Fig. 1 shows SDSC curves obtained for PHB, with 2 °C min^{-1} average heating rate after treatment by cooling at 2 °C min^{-1}. SDSC results of the raw heat flow, apparent thermodynamic C_p and IsoK baseline curves (curves a, b and c respectively) are shown in this figure. The thermodynamic C_p curve, which is similar to a reversing C_p shows the temperature dependence of specific heat and reversing latent heat changes during heating. The IsoK baseline, similar to non-reversing C_p, represents the kinetic changes of the PHB [12]. Both IsoK baselines [heat capacity (curve d) and heat flow (curve c)] reveal that PHB undergoes some recrystallisation during melting, as evidenced by small exothermic peaks (indicated by an arrow). As in other TMDSC methods, the endothermic melting is also evident in both $C_{p,\mathrm{IsoK}}$ and $C_{p,\mathrm{ATD}}$ curves [12,16]. The double or multiple melting behaviour of PHB has been known and suggested to be attributed to secondary crystallisation, which can occur during the melting process as well as during storage at room temperatures [2,17]. The SDSC data provided clear evidence of the presence of melting–recrystallisation–remelting.

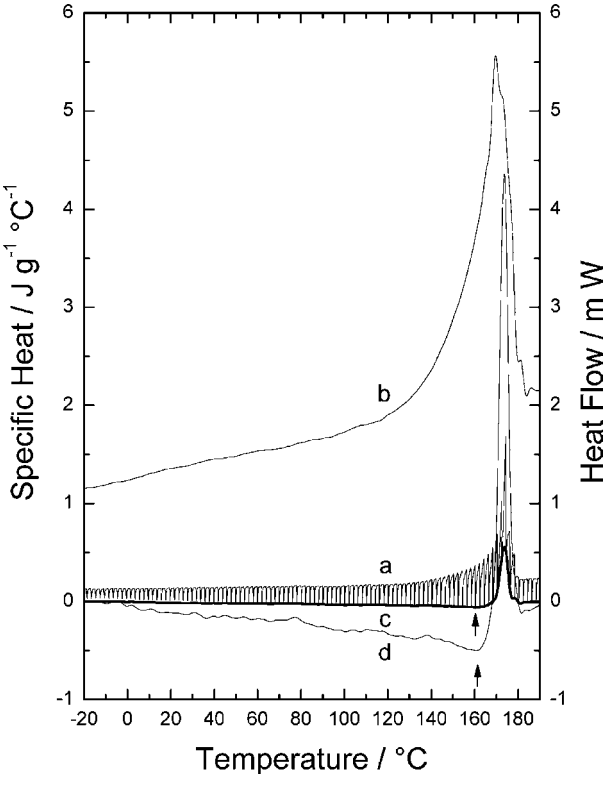

Fig. 1. (a) Raw heat flow, (b) apparent thermodynamic C_p, (c) IsoK baseline heat flow (thick line) and (d) IsoK baseline C_p of 2 °C min^{-1} cooled PHB from SDSC.

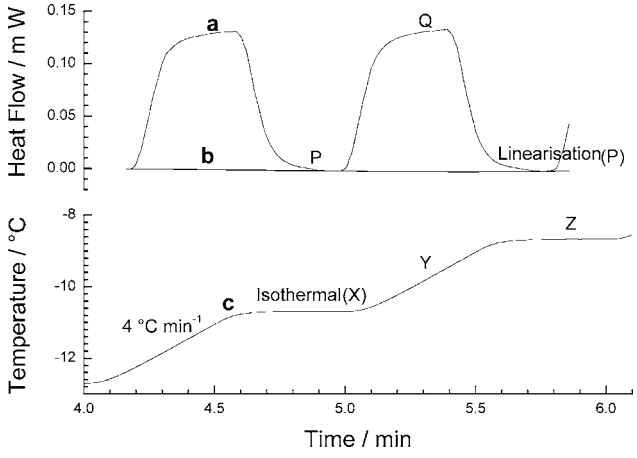

Fig. 2. SDSC method and resulting: (a) heat flow, (b) IsoK baseline and (c) temperature profiles.

The baseline subtracted heat flow, IsoK baseline and sample temperature versus time plots (curves a, b and c respectively) are shown for PHB in Fig. 2. In the SDSC method, each linear heating segment is immediately followed by an isothermal temperature segment (signal X). The DSC increased the temperature to new value at a selected heating rate (signal Y, at 4 °C min^{-1}), after which it was again held isothermally at a higher temperature (signal Z). The sample heat flow response approached equilibrium until the predetermined criteria (0.005 mW s^{-1}) was satisfied during each isothermal segment (segment P). The sample absorbed heat from its surroundings during the heating segments and the heat flow increased (segment Q). The method then repeated the previous two method segments, and each time the temperature progressively increased. Fig. 2 shows the linearisation region that was used to calculate the IsoK baseline (curve b) during isothermal segments. The thermodynamic C_p values were calculated from the area between the heat flow and the IsoK baseline during each heating segment.

3.2. Effect of hydroxyvalerate content

PHB, PHB5HV, PHB8HV and PHB12HV crystallised at a 2 °C min^{-1} rate from 190 to −20 °C were analysed by conventional DSC (Fig. 3) and SDSC melting scans with 2 °C min^{-1} average heating rate. Fig. 4 displays the $C_{p,\mathrm{ATD}}$ and $C_{p,\mathrm{IsoK}}$ curves obtained with an average heating rate of 2 °C min^{-1}. Corresponding thermal data, glass transition, cold crystallisation, melting temperatures and enthalpies obtained from $C_{p,\mathrm{ATD}}$ and $C_{p,\mathrm{IsoK}}$ curves are listed in Table 1. Melting temperatures and enthalpies were obtained from conventional DSC scans at a heating rate 2 °C min^{-1}, and these conventional DSC curves were used to calculate crystallinity of the polymers (Table 1).

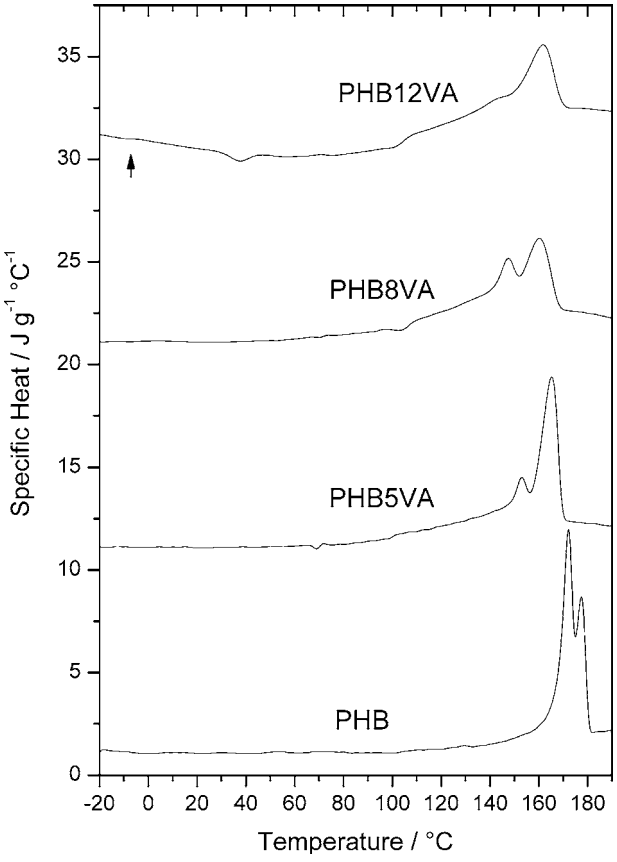

Fig. 3. Conventional DSC curves of PHB and its copolymers after cooling at 2 °C min^{-1}, for separation 10 units were added to each curve.

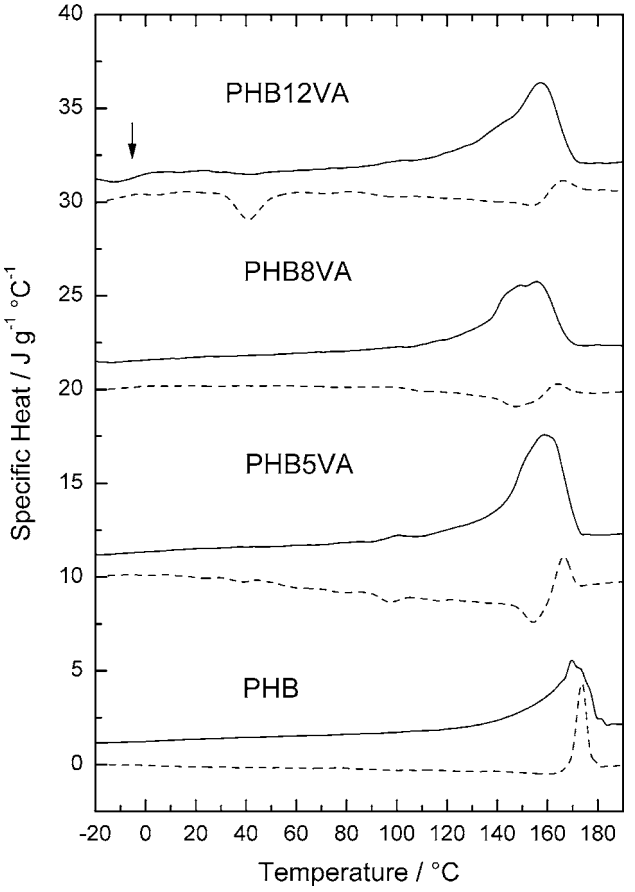

Fig. 4. SDSC curves of PHB and its copolymers after cooling at 2 °C min^{-1}. $C_{p,\mathrm{ATD}}$ curves (full) and IsoK baseline (dashed), for separation 10 units were added to each curve.

Unresolved double melting peaks were observed in the range of 144.2–177.9 °C for each polymer scanned by the conventional DSC program. PHB displayed a lower temperature melting peak at 172.4 °C due to melting of primary crystals and a higher shoulder at 177.9 °C that was attributed to the melting of recrystallised crystals. Furthermore, the smaller area of the second melting peak indicated that the amount of recrystallised crystals was smaller compared with the primary crystals. The copolymers showed double melting peaks with lower melting temperatures than the melting temperatures of PHB (Table 1). In contrast to PHB the smaller areas of the lower melting peaks were attributed to the amount of primary crystals, which was smaller than the recrystallised crystals in the copolymers. The highest crystallinity was 0.62 for PHB, lower crystallinities of 0.58, 0.51, and 0.47 were obtained for PHB5HV, PHB8HV and PHB12HV copolymers respectively. In the case of bacterial PHBHV, it is well known that the minor comonomer unit is excluded in the crystal lattice

Table 1
Thermal data for PHB and its copolymers with various hydroxyvalerate contents

Polymer	T_m (total) (°C)	ΔH_m (total) (J g^{-1})	T_g ($C_{p,\mathrm{ATD}}$) (°C)	T_m ($C_{p,\mathrm{ATD}}$) (°C)	ΔH_m ($C_{p,\mathrm{ATD}}$) (J g^{-1})	T_{cc} ($C_{p,\mathrm{IsoK}}$) (°C)	ΔH_{cc} ($C_{p,\mathrm{IsoK}}$) (J g^{-1})	T_m ($C_{p,\mathrm{IsoK}}$) (°C)	ΔH_m ($C_{p,\mathrm{IsoK}}$) (J g^{-1})	X_c[a]
SC2-PHB	172.4 177.9	90.1	–	169.6 172.8	116.0	–	–	173.8	21.3	0.62
SC2-PHB5VA	152.9 165.5	84.7	–	150.5 158.6	121.2	–	–	166.5	10.1	0.58
SC2-PHB8VA	147.6 160.2	74.6	–	143.4 155.6	103.8	–	–	163.5	4.0	0.51
SC2-PHB12VA	144.2 163.3	69.0	−3.9	140.2 157.2	126.6	41.0	36	166.2	3.9	0.47

SC2-PHB: 2 °C min^{-1} cool PHB, SC2-PHB5VA: 2 °C min^{-1} cool PHB5VA, SC2-PHB8VA: 2 °C min^{-1} cool PHB8VA, SC2-PHB12VA: 2 °C min^{-1} cool PHB12VA.

[a] Crystallinity was calculated using ΔH_m (total) curve.

of the major comonomer unit. The minor comonomer unit would interrupt the crystallisation behaviour of the major comonomer component and the former is excluded from the crystalline region, resulting in a decreased degree of crystallinity [18].

PHB and its copolymers crystallised at a rate of 2 °C min^{-1} were studied using SDSC. Fig. 4 displays the $C_{p,\mathrm{ATD}}$ and $C_{p,\mathrm{IsoK}}$ specific heat capacity curves derived from the SDSC iso-scan heating scans. The melting transitions can be seen in each curve. The $C_{p,\mathrm{ATD}}$ curve of PHB shows one melting peak with shoulder that emerged from the higher temperature side, while the $C_{p,\mathrm{IsoK}}$ shows a broad exothermic peak before melting (at about 165 °C, indicated by an arrow) and a sharp melting endotherm at 173.8 °C. Analogous melting behaviour was observed in the $C_{p,\mathrm{ATD}}$ curves of both PHB5HV and PHB8HV showing one melting peak with a shoulder on the lower temperature side of the peak, whereas the $C_{p,\mathrm{IsoK}}$ showed a broad exothermic peak before melting followed by an endothermic peak. In contrast, the $C_{p,\mathrm{ATD}}$ curve of PHB12HV showed a glass transition temperature of −3.9 °C and broad melting peak with a shoulder on the lower temperature side. The $C_{p,\mathrm{IsoK}}$ showed a cold crystallisation peak at 41 °C, a broad exothermic peak (marked on the curve) and one melting endotherm. This sample with the highest HV content showed increasing amorphous behaviour, due to the greater comonomer exclusion from crystals.

As mentioned previously, the $C_{p,\mathrm{ATD}}$ provides the reversing component of the total heat capacity, whereas the $C_{p,\mathrm{IsoK}}$ represents the non-reversing component of the total heat capacity, similar to reversing and non-reversing signals of the Fourier transformation-based TMDSC iso-scan method [19]. The exothermic only or both endothermic and exothermic behaviour of the non-reversing C_p curve of TMDSC has been observed for other polymers such as poly(ethylene-2,6-napthalene dicarboxylate) [20,21] and polyethylenes [22] depending on crystal stability.

The exothermic peak of non-reversing curves in Fig. 4 suggested that PHB and its copolymers with HV provided significant recrystallisation and/or annealing throughout the SDSC heating process. Due to the overlay of the recrystallisation exotherm and the melting endotherm, the recrystallisation exotherm is not observed in a conventional DSC scan. The reversing contribution was considerably decreased with increased of HV content, which formed thinner lamella, though at a slower rate as indicated by the crystallisation exotherm of PHB12HV. Wunderlich et al. have reported that poorly crystallised polymers have a larger reversing melting contribution and smaller non-reversing contribution, while perfect crystals exhibit only a small reversing and a larger non-reversing contribution [6]. Endothermic melting can be observed in both reversing and non-reversing C_p curves, but exothermic behaviour was detected only in the non-reversing C_p curve because the slow crystallisation kinetics caused a heat flow response, which is not in-phase with the temperature oscillation of the TMDSC scan [6]. Similar behaviour can be detected in $C_{p,\mathrm{ATD}}$ and $C_{p,\mathrm{IsoK}}$ specific heat capacity curves obtained from SDSC scans of PHB and its copolymers.

Under an iso-scan SDSC heating program, which contains a sequence of heating and isothermal steps, the polymer has the opportunity to melt and recrystallise during the isothermal conditions at a series of increasing isothermal temperatures. Thus, the polymers heated by the iso-scan program had greater equilibration time than the polymers analysed by conventional DSC (continuous heating) method, since the iso-scan method allowed more time for the rearrangement of unstable crystals. Therefore, the increased enthalpy observed by SDSC scans of PHB and its copolymers was attributed to crystal perfection during the isothermal steps.

$C_{p,\mathrm{ATD}}$ curves of all polymers showed unresolved double melting peaks, whereas $C_{p,\mathrm{IsoK}}$ data demonstrated exothermic peaks in the melting region suggesting the presence of a melting–recrystallisation–remelting (mrr) process. As mentioned before, endothermic melting was also observed in the $C_{p,\mathrm{IsoK}}$. As the HV content increased, T_m of copolymers was shifted towards a lower temperature (Table 1). The shift of T_m to a lower temperature and lower crystallinity suggest that the copolymers contain thinner lamellar crystals due to the higher comonomer content. The slight shift in the shape of the melting peak to lower temperatures suggests crystallites (lamella) with reduced thermal stability had been formed [23].

The double or multiple melting behaviours are common for PHB and its copolymers depending on the crystallisation conditions [24]. Multiple melting behaviour of a polymer is usually proposed to link either to the process of mrr or to melting of crystals with different lamellar thickness and/or different crystal morphology [25]. It has been shown that the mrr process operated for melt crystallised PHB and its copolymers with various hydroxyvalerate content. The data suggested that the extent of recrystallisation during heating was less for slow-cooled polymers. At a slow cooling rate, all these polymers except PHB12HV may form relatively well-organised lamellae, which undergo less rearrangement.

3.3. Influence of crystallisation conditions

Fig. 5 displays $C_{p,\mathrm{ATD}}$ and $C_{p,\mathrm{IsoK}}$ curves calculated from SDSC heating scans of PHB5HV obtained at an average heating rate of 2 °C min^{-1} after cooling at rates of 200, 20 and 2 °C min^{-1}. The corresponding thermal data, glass transition, cold crystallisation and melting temperatures, enthalpies and crystallinity, are listed in Table 2. As expected, the reversible event of T_g (as indicated by an arrow) is shown in the $C_{p,\mathrm{ATD}}$ curves as a step change although irreversible effects, cold crystallisation exothermic peaks and the recrystallisation peaks, are present in the $C_{p,\mathrm{IsoK}}$ curves. A single melting peak was observed for all crystallisation conditions, except for the sample cooled at 2 °C min^{-1}. The slow-cooled PHB5HV showed a melting peak with a shoulder that emerged from the lower temperature side of the melting peak (as indicated by an arrow). The sample cooled at a 2 °C min^{-1} had the lowest T_m

Table 2
SDSC thermal data for PHB5HV treated by different cooling treatments

Polymer	T_g (C_p,ATD) (°C)	T_m (C_p,ATD) (°C)	ΔH_m (C_p,ATD) (J g^{-1})	T_{cc} (C_p,IsoK) (°C)	ΔH_{cc} (C_p,IsoK) (J g^{-1})	T_m (C_p,IsoK) (°C)	ΔH_m (C_p,Isok) (J g^{-1})
FC200-PHB5VA	−2.6	159.9	110.4	31.8	17.4	167.0	8.4
MC20-PHB5VA	−2.3	159.8	114.4	31.5	17.5	167.1	8.2
SC2-PHB5VA		158.6 150.5	121.2	–	–	166.5	10.1

FC200-PHB5VA: 200 °C min^{-1} cool PHB5VA, MC20-PHB5VA: 20 °C min^{-1} cool PHB5VA, SC2-PHB5VA: 2 °C min^{-1} cool PHB5VA.

value (158.6 °C) and a shoulder at 150.5 °C, while PHB5HV crystallised at 20 and 200 °C min^{-1} showed a higher melting peak at 159.9 °C. As the cooling rate increased, melting peaks were shifted towards higher temperatures and peaks became broader indicating the melting may be accompanied by recrystallisation for the PHB5HV crystallised at faster rates. The recrystallisation caused the development of a second melting peak during the SDSC heating scan, while the first melting peak was due to melting of primary crystals.

According to the thermal data in Table 2, the PHB5HV sample crystallised at 2 °C min^{-1} rate had the highest crystallinity of 0.83 and the 200 °C min^{-1} cooled PHB5HV sample had the lowest crystallinity (0.76). Both 20 and 200 °C min^{-1} cooled PHB5HV show a glass transition as marked on the curves at −2.6 and −2.3 °C respectively and an exothermic cold crystallisation peak (T_{cc}) at ∼32 °C, confirming more amorphous polymer during the fast-cooled treatments [26]. In contrast, the highly crystalline PHB5HV that was crystallised at a rate of 2 °C min^{-1} showed no T_g or cold crystallisation peaks in the $C_{p,ATD}$ or $C_{p,IsoK}$ curves under non-isothermal cooling conditions, the fraction and perfection of crystals was controlled by the cooling rate. The increased crystallinity of 2 °C min^{-1} cooled polymer may be due to the recrystallised and/or annealed PHB5HV crystals during the SDSC melting scan.

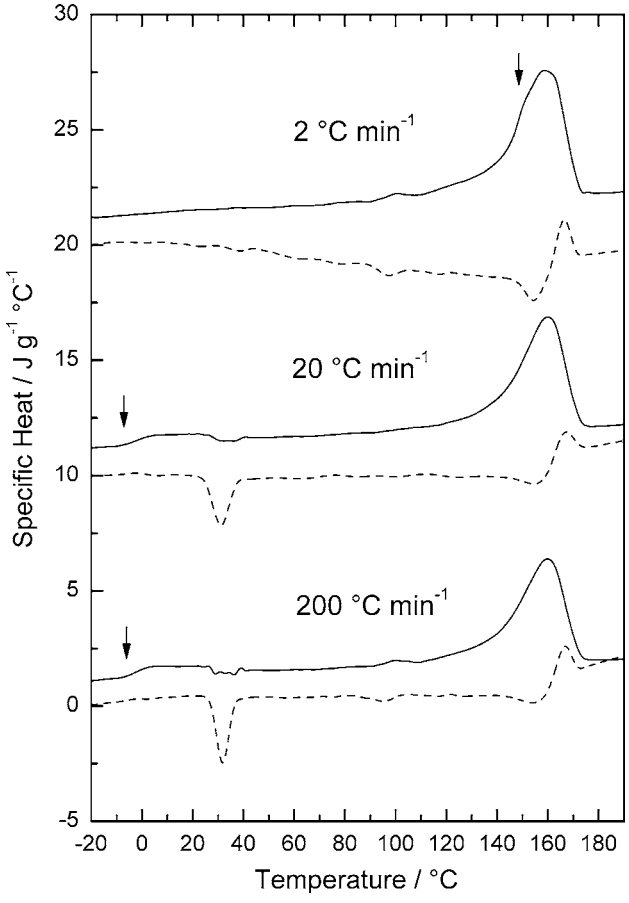

Fig. 5. SDSC curves of PHB5HV after different cooling treatments; cooling rates are shown on the curves. $C_{p,ATD}$ curves (full) and $C_{p,IsoK}$ (dashed), for separation 10 units were added to each curve.

3.4. Morphological studies

The crystal morphology of PHB5HV was observed by polarised optical microscopy after isothermally, slow and fast cooling crystallisation conditions. As illustrated in Fig. 6, different crystal morphologies were obtained under various crystallisation conditions. All images showed the characteristic larger spherulites that contain a Maltese cross-birefringent pattern and concentric extinction bands [27]. A sharp fibril structure growing radially with a large radius was seen for isothermally crystallised PHB5HV at 80 °C (Fig. 6a). Fig. 6b and c shows the polarised optical microscopy images of PHB cooled at 2 and 20 °C min^{-1} from 140 °C and 5 °C min^{-1} to 140 °C from the melt respectively. These cooling treatments were performed analogous to the DSC cooling treatments of this polymer (curves for 2 and 20 °C min^{-1}).

Slow cooling initiated crystallisation at a higher temperature with low nucleation density permitting large crystals to grow, whereas faster cooling resulted in smaller crystal size induced by increased nucleation density. Thus, the slow-cooled polymers have larger spherulites than fast-cooled polymers. Banded spherulites were observed for all copolymers and the sizes of the spherulites of continuous cooled polymers were smaller than when isothermally crystallised. The improved mechanical properties and thermal behaviour of PHB copolymers are attributed to the spherulite growth [28]. These findings are consistent with the large individual spherulites of PHB and its copolymers

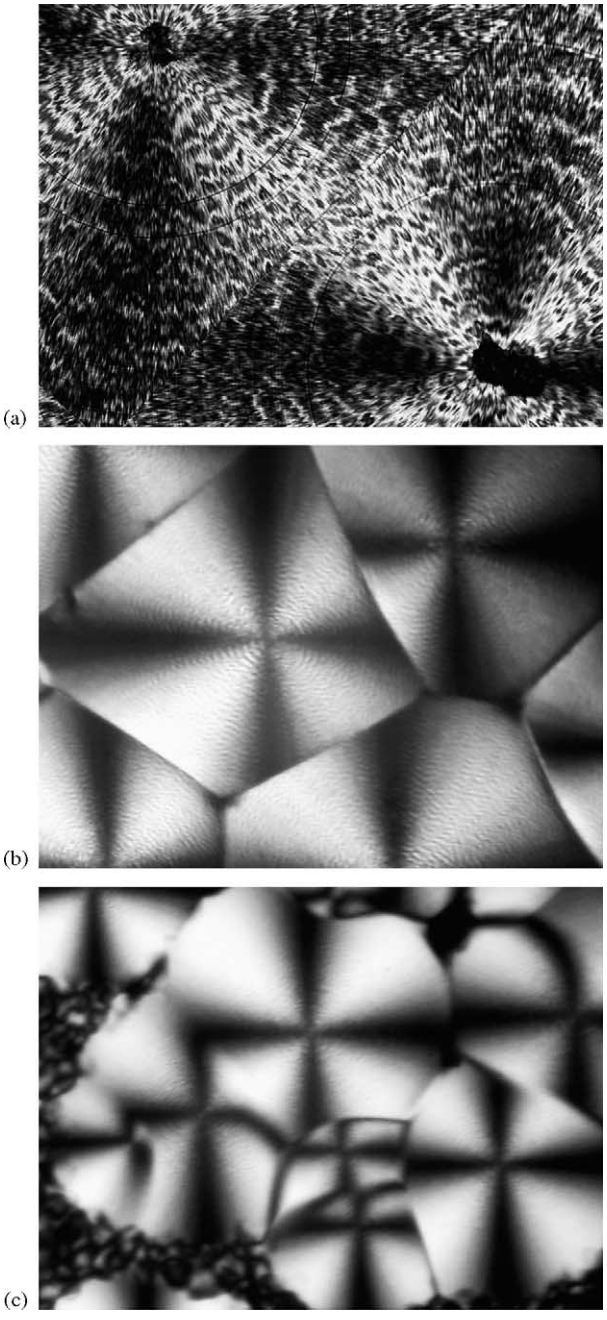

Fig. 6. Polarised optical microscopy images (100×) of: (a) PHB5HV after isothermal crystallisation at 80 °C, (b) PHB5HV cooling at 2 °C min^{-1} and (c) PHB5HV cooling at 20 °C min^{-1}.

previously observed [2,27]. Separation of bands and regularity of bands varied with crystallisation temperatures and conditions [29]. Isothermal and slow-cooled polymers provided a large average spherulite radius indicating a low nucleation density [30]. It is these large spherulites that are responsible for the brittleness of copolymers of PHB with low HV content [31]. These results provided clear evidence of crystal growth dependence of PHB5HV on crystallisation conditions.

4. Conclusion

The SDSC approach has proved valuable in the interpretation of melting of PHB and PHBHV copolymers. The results have interpreted multiple melting peak behaviour and the increased degree of crystallinity of melt–slow-cooled polymers as due to the melt–recrystallisation process occurring during subsequent heating. This phenomenon was evidenced by the irreversible effects shown by exothermic peaks in $C_{p,\mathrm{IsoK}}$ and reversing events in the $C_{p,\mathrm{ATD}}$ signals, which cannot be obtained by standard DSC analysis. The influence of HV content in the copolymers of PHB was revealed by the SDSC method. The SDSC method separated reversing and non-reversing contribution without Fourier transformation, by step-wise measurement of specific heat.

Acknowledgement

L.M.W.K. Gunaratne acknowledges financial support of a postgraduate scholarship from RMIT University.

References

[1] C.-S. Ha, W.-J. Cho, Prog. Polym. Sci. 27 (2002) 759.
[2] A. EI-Hadi, R. Schanabel, E. Straube, G. Muller, S. Henning, Polym. Testing 21 (2002) 665.
[3] S. Peng, Y. An, C. Chen, B. Fei, Y. Zhuang, L. Dong, Eur. Polym. J. 39 (2003) 1475.
[4] P.S. Gill, S.R. Sauerbrunn, M. Reading, J. Therm. Anal. Calorim. 40 (1993) 931.
[5] J.E.K. Schawe, Thermochim. Acta 260 (1995) 1.
[6] B. Wunderlich, I. Okazaki, K. Ishikiriyama, A. Boller, Thermochim. Acta 324 (1998) 77.
[7] B. Wunderlich, A. Boller, I. Okazaki, K. Ishikiriyama, W. Chen, M. Pyda, J. Pak, I. Moon, R. Androsch, Thermochim. Acta 330 (1999) 21.
[8] Y.G. Jeong, W.H. Jo, S.C. Lee, Polymer 44 (2003) 3259.
[9] C.-L. Wei, M. Chen, F.-E. Yu, Polymer 44 (2003) 8185.
[10] G. Amarasinghe, F. Chen, A. Genovese, R.A. Shanks, J. Appl. Polym. Sci. 90 (2003) 681.
[11] W.J. Sichina, R.B. Cassel, Proceedings of the 28th NATAS Conference, Orlando, FL, 2000, p. 158.
[12] K. Pielichowski, K. Flejtuch, J. Pielichowski, Polymer 45 (2004) 1235.
[13] M. Sandor, N.A. Bailey, E. Mathiowitz, Polymer 43 (2003) 279.
[14] L.L. Zhang, S.H. Goh, S.Y. Lee, G.R. Hee, Polymer 41 (2000) 1429.
[15] S. Gogolewski, M. Jovanovic, S.M. Perren, J.G. Dillon, M.K. Hughes, J. Biomed. Mater. Res. 27 (1993) 1135.
[16] B.B. Sauer, W.G. Kampert, E. Neal Blanchard, S.A. Threefoot, B.S. Hsiao, Polymer 41 (2000) 1099.
[17] G.J.M. De Konig, P.J. Lamstra, Polymer 34 (1993) 4089.
[18] S. Yamada, Y. Wang, N. Asakawa, N. Yoshie, Y. Inoue, Macromolecules 34 (2001) 4659.
[19] L.M.W.K. Gunaratne, R.A. Shanks, G. Amarasinghe, Thermochim. Acta 423 (2004) 127.
[20] B.B. Sauer, W.G. Kamper, E. Neal Blanchard, SA. Threefoot, B.S. Hsiao, Polymer 41 (2000) 1099.
[21] W.G. Kampert, B.B. Sauer, Polymer 42 (2001) 8703.
[22] J. Pak, B. Wunderlich, Macromolecules 34 (2001) 4492.
[23] F. Gassner, A.J. Owen, Polym. Int. 39 (1996) 215.

[24] R. Pearce, R.H. Marchessault, Polymer 35 (1994) 3990.
[25] V.B.F. Mathot (Ed.), Calorimetry and Thermal Analysis of Polymers, Hanser, New York, 1993, Chapter 9, p. 231.
[26] R. Renstad, S. Karlsson, A.-C. Albertsson, P.-E. Werner, M. Westdahl, Polym. Int. 43 (1997) 201.
[27] F. Biddlestone, A. Harris, J.N. Hay, Polym. Int. 39 (1996) 221.
[28] C. Chen, B. Fei, S. Peng, H. Wu, Y. Zhuang, X. Chen, L. Dong, Z. Feng, J. Polym. Sci. B: Polym. Phys. 40 (2002) 1893.
[29] A. Keller, H.H. Willis, J. Polym. Sci. XXXIX (1959) 151.
[30] M. Gazzano, M.L. Focarete, C. Reikel, A. Ripamonti, M. Scandola, Macromol. Chem. Phys. 202 (2001) 1405.
[31] P.J. Barham, A. Keller, J. Polym. Sci., Polym. Phys. Edit. 24 (1986) 69.